STRUCTURAL CHEMISTRY

ISSN 2053-2296

Monoprotonated species of 2-aminomalonyl difluoride, $[C_3H_4F_2NO_2][H_2F_3]$

Dirk Hollenwäger,* Dominik Leitz, Valentin Bockmair and Andreas J. Kornath‡

Department Chemie, Ludwig-Maximilians Universität, Butenandtstrasse 5-13 (Haus D), D-81377 München, Germany.
*Correspondence e-mail: dirk.hollenwaeger@cup.uni-muenchen.de

Received 4 October 2024
Accepted 25 December 2024

Edited by T. Ohhara, J-PARC Center, Japan Atomic Energy Agency, Japan

‡ Deceased

Keywords: crystal structure; 2-aminomalonyl difluoride; aminoacyl fluoride; vibrational spectroscopy; sulfur tetrafluoride; complexone.

CCDC reference: 2413368

Supporting information: this article has supporting information at journals.iucr.org/c

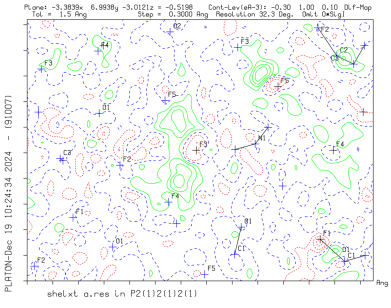

The monoprotonated species of 2-aminomalonyl difluoride, namely, 1,3-difluoro-1,3-dioxopropan-2-aminium dihydrogen trifluoride, $[C_3H_4F_2NO_2][H_2F_3]$, was synthesized from sulfur tetrafluoride in anhydrous hydrogen fluoride (aHF) with $[NH_4][C_3H_5NO_4]$ as the starting material. The solvent was removed and the salt was dissolved in aHF and crystallized. In the solid state, the three-dimensional network is built by medium–strong N—H···F hydrogen bonds and C···F contacts. This is the first structure determination of an aminoacyl difluoride and the second of an aminoacyl fluoride.

1. Introduction

The monoprotonated species of 2-aminomalonyl difluoride, as the $[C_3H_4F_2NO_2][H_2F_3]$ salt, is the second characterized salt of an acylamino fluoride, after the synthesis of glycinoyl fluoride (Hollenwäger *et al.*, 2024*a*). Glycinoyl fluoride with protection groups was first characterized by NMR spectroscopy in 1999 by Carpino & Mansour (1999). The direct synthesis of acylamino fluorides was investigated by our group in 2024 (Hollenwäger *et al.*, 2024*a*). The solid state of glycinoyl fluoride was characterized by vibrational and NMR spectroscopy, as well as single-crystal X-ray diffraction (Hollenwäger *et al.*, 2024*a*). $[C_3H_4F_2NO_2]^+$ is the first cation of the group of acyl fluorides which contains two acyl fluoride moieties. The direct synthesis with sulfur tetrafluoride in anhydrous hydrogen fluoride (aHF) applies Kollonitsch's idea of using HF as a solvent to improve the formation of SF_3^+ to activate the deoxyfluorinating species (Kollonitsch *et al.*, 1975). The aHF also performs the function of protonating the NH_2 group to prevent adduct formation of SF_4 with the lone pair of the nitrogen (Hollenwäger *et al.*, 2024*a*; Goettel *et al.*, 2012; Chaudhary *et al.*, 2015). $[C_3H_4F_2NO_2][H_2F_3]$ is produced with $[NH_4][C_3H_5NO_4]$ as the starting material and belongs to the group of complexones (Hollenwäger *et al.*, 2024*b*; Anderegg *et al.*, 2005). Due to the high toxicity of fluoride, its application is highly likely to be limited. The salt could be used in the specialized field of fluorine chemistry, as its two acyl fluoride moieties make it highly interesting for conversion in superacidic or Lewis acidic media.

2. Experimental

2.1. Synthesis and crystallization

$[NH_4][C_3H_5NO_4]$ (67 mg, 0.893 mmol) was added in an FEP (fluorinated ethylene propylene) tube reactor. Anhydrous hydrogen fluoride (aHF, 0.75 ml) and sulfur tetrafluoride (203 mg, 1.87 mmol) were then added at −196 °C, and the

mixture homogenized at room temperature. Excess solvent was removed at −78 °C overnight. The product was a colourless solid that was stable at room temperature. The equation of the formation is shown in Scheme 1.

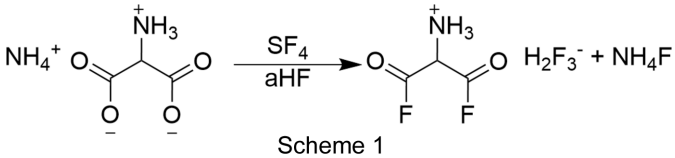

Scheme 1

2.2. Analysis (X-ray and Raman)

We investigated and characterized the $[C_3H_4F_2NO_2][H_2F_3]$ salt by single-crystal X-ray diffraction and Raman spectroscopy. Complete data and the devices used for the X-ray measurements are listed in the supporting information (CIF file). Low-temperature Raman spectroscopic studies were performed using a Bruker MultiRAM FT–Raman spectrometer with Nd:YAG laser excitation (λ = 1064 cm^{-1}) under vacuum at −196 °C. For measurements, the synthesized compounds were transferred to a cooled glass cell.

2.3. Refinement

Crystal data, data collection and structure refinement details are summarized in Table 1. The positions of the H atoms were identified by residual electron-density peaks on the difference Fourier map and by evaluation of the contacts (Fig. 1). Due to the high diffraction resolution, all H atoms were assigned with respect to the difference map and freely refined.

Table 1
Experimental details.

Crystal data	
Chemical formula	$C_3H_3F_2NO_2^+·H_2F_3^-$
M_r	183.09
Crystal system, space group	Orthorhombic, $P2_12_12_1$
Temperature (K)	102
a, b, c (Å)	5.5736 (2), 9.2154 (4), 12.7952 (7)
V (Å^3)	657.20 (5)
Z	4
Radiation type	Mo $K\alpha$
μ (mm^{-1})	0.23
Crystal size (mm)	0.34 × 0.11 × 0.07
Data collection	
Diffractometer	Rigaku Xcalibur Sapphire3
Absorption correction	Multi-scan (*CrysAlis PRO*; Rigaku OD, 2020)
T_{min}, T_{max}	0.945, 1.000
No. of measured, independent and observed [$I > 2\sigma(I)$] reflections	7118, 2187, 1930
R_{int}	0.034
$(\sin\theta/\lambda)_{max}$ (Å^{-1})	0.752
Refinement	
$R[F^2 > 2\sigma(F^2)]$, $wR(F^2)$, S	0.034, 0.067, 1.02
No. of reflections	2187
No. of parameters	124
H-atom treatment	All H-atom parameters refined
$\Delta\rho_{max}$, $\Delta\rho_{min}$ (e Å^{-3})	0.27, −0.18
Absolute structure	Flack x determined using 683 quotients $[(I^+) - (I^-)]/[(I^+) + (I^-)]$ (Parsons *et al.*, 2013)
Absolute structure parameter	−0.3 (5)

Computer programs: *CrysAlis PRO* (Rigaku OD, 2020), *SHELXT* (Sheldrick, 2015*a*), *SHELXL2019* (Sheldrick, 2015*b*), *ORTEP-3 for Windows* (Farrugia, 2012) and *PLATON* (Spek, 2020).

3. Results and discussion

3.1. Single-crystal X-ray diffraction

Herein we present the results of the single-crystal X-ray diffraction study of the salt $[C_3H_4F_2NO_2][H_2F_3]$, namely, monoprotonated 2-aminomalonyl difluoride dihydrogen trifluoride. The salt crystallizes in the orthorhombic space group $P2_12_12_1$ with four formula units per unit cell. The asymmetric unit is shown in Fig. 2. The C1—C3 [1.518 (2) Å] and C2—C3 [1.519 (2) Å] bonds are shortened compared to those of the starting material [1.539 (2) and 1.549 (2) Å, respectively; Hollenwäger *et al.*, 2024*b*]. The C—C bond lengths are elongated compared to the electron diffraction values of malonyl difluoride [1.502 (5) Å; Jin *et al.*, 1992]. The C1—F1 bond length [1.331 (2) Å] is in the same range as the C2—F2 bond [1.329 (2) Å]. Compared to the C—F bond length of malonyl difluoride (Jin *et al.*, 1992), the bond in $[C_3H_4F_2NO_2][H_2F_3]$ [1.349 (4) Å] is slightly shortened. The C═O bonds [C1═O1 = 1.175 (2) Å and C1═O2 = 1.172 (2) Å] are in the same range as in malonyl difluoride [1.177 (3) Å; Jin *et al.*, 1992]. The C3—N1 bond length [1.469 (2) Å] is significantly shortened with respect to the starting material [1.482 (2) Å], the Csp^3—Nsp^3 bond lengths (1.488 Å) in organic compounds and the bond in glycine [1.482 (3) Å; Hollenwäger *et al.*, 2024*b*; Allen *et al.*, 1987; Jiang *et al.*, 2015]. Table 2 lists the bond lengths, bond angles and torsion angles of the $[C_3H_4F_2NO_2][H_2F_3]$ salt, the starting material $[NH_4][C_3H_5NO_4]$, glycinoyl fluoride, β-glycine and malonyl difluoride (Hollenwäger *et al.*, 2024*a*,*b*; Jiang *et al.*, 2015; Jin *et al.*, 1992). The bond deviation of the crystal structure of

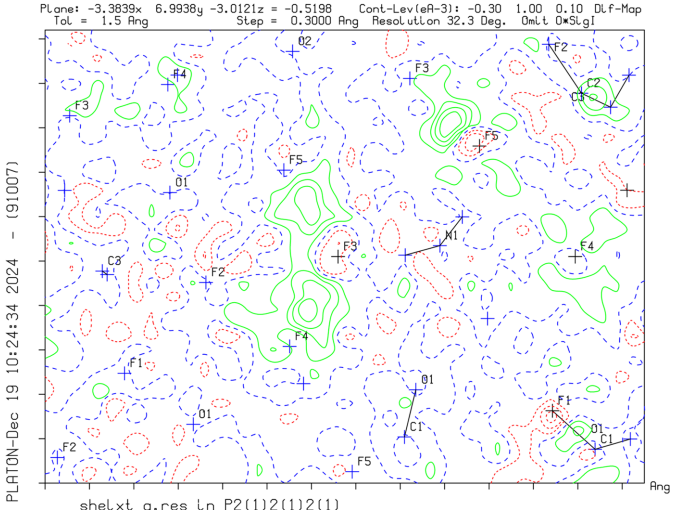

Figure 1
A difference Fourier map of $[C_3H_4F_2NO_2][H_2F_3]$ without the H atoms between F3, F4 and F5, and between N1 and F3, F4 and F5. The green solid lines and red dotted lines show positive and negative density distribution, respectively.

Table 2
Bond lengths (Å), bond angles (°) and torsion angles (°) of $[C_3H_4F_2NO_2][H_2F_3]$, $[NH_4][C_3H_5NO_4]$, glycinoyl fluoride, *β*-glycine and malonyl difluoride.

Bond length	$[C_3H_4F_2NO_2][H_2F_3]$	$[NH_4][C_3H_5NO_4]$	Glycinoyl fluoride	*β*-Glycine	Malonyl difluoride
C1—C3	1.518 (2)	1.5394 (18)	1.509 (5)	1.536 (3)	1.502 (5)
C2—C3	1.519 (2)	1.5485 (18)			1.502 (5)
C1—F1	1.331 (2)		1.333 (4)		1.349 (4)
C2—F2	1.329 (2)				1.349 (4)
C1═O1	1.175 (2)	1.2483 (16)		1.257 (2)	1.177 (3)
C2═O2	1.172 (2)	1.2462 (17)		1.258 (3)	1.177 (3)
C3—N1	1.469 (2)	1.4821 (16)	1.476 (5)	1.482 (3)	
Angle					
C1—C2—C3	114.1 (1)	113.00 (10)			110.2 (10)
C3—C1—O1	126.0 (2)	117.7 (1)	127.2 (3)		129.1 (8)
C3—C2—O2	125.9 (2)	116.9 (1)			129.1 (8)
C3—C1—F1	111.3 (1)		110.2 (3)		109.7 (7)
C3—C2—F2	111.4 (1)				109.7 (7)
N1—C3—C1	108.5 (1)	109.56 (10)	108.3 (3)	111.8 (1)	
N1—C3—C2	108.6 (1)	109.98 (10)			
Torsion angle					
F1—C1—C3—N1	−173.5 (1)				
F1—C1—C3—C2	65.4 (2)				
O1—C1—C3—N1	4.7 (2)	−2.96 (16)	8.1 (5)		
O1—C1—C3—C2	−116.4 (2)	120.0 (1)			112.0 (20)
F2—C2—C3—N1	177.7 (1)		−171.2 (3)		
F2—C2—C3—C1	−61.2				
O2—C2—C3—C1	122.4 (2)	−112.3 (1)			0.0

$[C_3H_4F_2NO_2][H_2F_3]$ with respect to malonyl difluoride results from the structure of malonyl difluoride being measured in the gas phase (Jin *et al.*, 1992). The shortened C—C bond lengths of the $[C_3H_4F_2NO_2][H_2F_3]$ salt compared to the $[NH_4][C_3H_5NO_4]$ salt is a result of the stronger negative inductive effect of fluorine compared to oxygen in the carboxylic acid. Additionally, the starting material is a zwitterionic anion and the shown aminoacyl fluoride is a cationic salt. The determined structures of glycinoyl fluoride and $[C_3H_4F_2NO_2][H_2F_3]$ are in good agreement with each other (Hollenwäger *et al.*, 2024*a*). The second acyl fluoride moiety of $[C_3H_4F_2NO_2][H_2F_3]$ also exerts a negative inductive effect on the backbone, whereby the C—C bonds are slightly lengthened compared to glycinoyl fluoride (Hollenwäger *et al.*, 2024*a*).

The C—C—C angle [114.1 (1)°] is significantly increased compared to both the starting material [113.0 (1)°] and malonyl difluoride [110.2 (10)°; Jin *et al.*, 1992; Hollenwäger *et al.*, 2024*b*]. The C—C—O angles [C3—C1—O1 = 126.0 (2)° and C3—C2—O2 = 125.9 (2)°] are significantly decreased compared to malonyl difluoride [129.1 (8)°; Jin *et al.*, 1992]. The C—C—F angles [111.4 (1) and 111.3 (1)°] are significantly increased compared to malonyl difluoride [109.7 (7)°; Jin *et al.*, 1992]. The C—C—N angles [N1—C3—C1 = 108.5 (1)° and N1—C3—C2 = 108.6 (1)°] are slightly decreased compared to

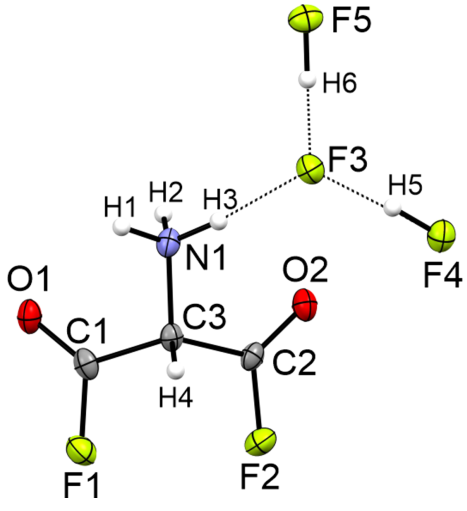

Figure 2
The asymmetric unit of $[C_3H_4F_2NO_2][H_2F_3]$, with displacement ellipsoids drawn at the 50% probability level.

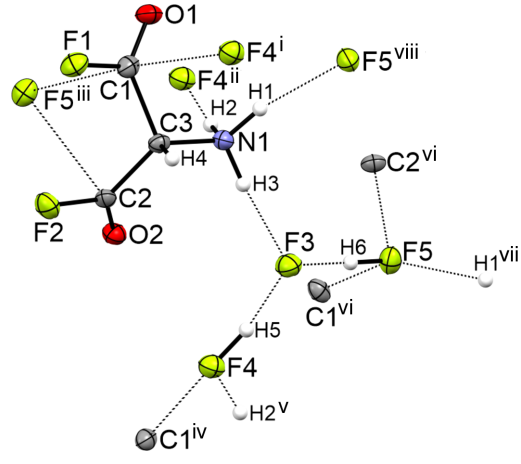

Figure 3
Hydrogen bonds in the crystal structure of $[C_3H_4F_2NO_2][H_2F_3]$, with displacement ellipsoids drawn at the 50% probability level. [Symmetry codes: (i) $-x+1, y-\frac{1}{2}, -z+\frac{1}{2}$; (ii) $x-1, y, -z$; (iii) $-x+\frac{1}{2}, -y+1, z-\frac{1}{2}$; (iv) $-x+1, y+\frac{1}{2}, -z+\frac{1}{2}$; (v) $x+1, y, z$; (vi) $-x+\frac{1}{2}, -y+1, z+\frac{1}{2}$; (vii) $x+\frac{1}{2}, -y+\frac{1}{2}, -z+1$; (viii) $x-\frac{1}{2}, -y+\frac{1}{2}, -z+1$.]

Table 3
Experimental (exptl) Raman vibrational frequencies (cm^{-1}) of $[C_3H_4F_2NO_2][H_2F_3]$ and calculated (calc) Raman vibrational frequencies (cm^{-1}) of $[C_3H_4NO_2F_2]^+$ at the M062x/aug-cc-pVTZ-level of theory (the scaling factor is 0.956).

Exptl	Calc		Assignment	
	3327 (173)	A	ν1	ν(NH)
3225 (6)	3182 (251)	A	ν2	ν(NH)
	3143 (67)	A	ν3	ν(NH)
2978 (19)	2980 (22)	A	ν4	ν(CH)
1877 (100)	1889 (297)	A	ν5	ν(CO)
1846 (31)	1862 (210)	A	ν6	ν(CO)
1627 (14)	1578 (34)	A	ν7	$\delta(NH_2)$
1611 (14)	1560 (44)	A	ν8	$\delta(NH_2)$
1378 (19)	1446 (187)	A	ν9	$\delta(NH_2)$
1303 (14)	1341 (251)	A	ν10	ν(CF)+δ(CH)
	1255 (98)	A	ν11	ν(CF)+δ(CH)
1235 (20)	1237 (208)	A	ν12	δ(CH)+ν(CF)
1152 (17)	1160 (59)	A	ν13	δ(CH)+ν(CF)
1133 (13)	1092 (43)	A	ν14	$\delta(CH)+\delta(NH_3)$
1083 (14)	1080 (8)	A	ν15	$\delta(CH)+\delta(NH_3)$
	1030 (16)	A	ν16	ν(CN)
923 (20)	895 (51)	A	ν17	ν(CC)
873 (47)	858 (25)	A	ν18	δ(CCC)
763 (77)	755 (1)	A	ν19	ν(CC)
657 (17)	650 (32)	A	ν20	δ(COF)
603 (20)	588 (3)	A	ν21	ρ(CCC)
587 (25)	576 (15)	A	ν22	$\delta(NH_3)$
533 (15)				
491 (36)				
475 (32)	486 (47)		ν23	$\delta(NH_3)$
439 (21)				
402 (34)	380 (18)	A	ν24	δ(CCF)
352 (43)	303 (14)	A	ν25	δ(CCF)
248 (20)	287 (14)	A	ν26	$\delta(NH_3)$
221 (41)				
203 (32)	191 (0)	A	ν27	$\delta(NH_3)$
155 (59)	160 (11)	A	ν28	δ(COF)
130 (55)				
99 (46)	93 (14)	A	ν29	τ(COF)
90 (47)				
80 (41)	45 (0)	A	ν30	τ(COF)

the starting material (Hollenwäger *et al.*, 2024*b*). The torsion angles are available in Table 2.

The crystal structure of $[C_3H_4F_2NO_2][H_2F_3]$ results from a three-dimensional network (Fig. 3) of two strong hydrogen bonds within the $[H_2F_3]^-$ anion [2.322 (2) Å for F4(—H5)···F3 and 2.338 (2) Å for F5(—H6)···F3] and three medium–strong hydrogen bonds classified according to Jeffrey (1997). The medium–strong hydrogen bonds connect the anion with the cation [2.655 (2) Å for N1(—H3)···F3, 2.742 (2) Å for N1(—H1)···F5 and 2.743 (2) Å for N1(—H2)···F4]. In addition, the network establishes three C···F contacts, which are within the van der Waals radii sum (3.17 Å) by approximately 16% [C1···F4 = 2.676 (2) Å, C1···F5 = 2.682 (2) Å and C2···F5 = 2.688 (2) Å]. The hydrogen bonds and C···F contacts are listed in the supporting information.

3.2. Raman spectroscopy

The low-temperature Raman spectra of $[C_3H_4F_2NO_2][H_2F_3]$, $[NH_4][C_3H_5NO_4]$ and $C_3H_4O_4$ are illustrated in Fig. 4. Table 3 lists the Raman data for $[C_3H_4F_2NO_2][H_2F_3]$ and the calculated frequencies for the $[C_3H_4F_2NO_2]^+$ cation at the aug-cc-pVTZ level of theory. The first evidence of the successful preparation of the $[C_3H_4F_2NO_2][H_2F_3]$ salt is the C═O valence oscillation being blue-shifted by approximately 193 cm^{-1} to 1877 and 1846 cm^{-1} compared to the starting material at 1684 cm^{-1} (Hollenwäger *et al.*, 2024*b*). The second pieces of evidence are the C—F valence oscillations, which are coupled with the δ(C—H) bands at 1303, 1235 and 1152 cm^{-1}. The C—C stretching vibrations are observed at 923 and 763 cm^{-1}. Only one of the three N—H vibrations is Raman-active and is observed at 3225 cm^{-1}. The C—H stretching oscillation is detected at 2978 cm^{-1}.

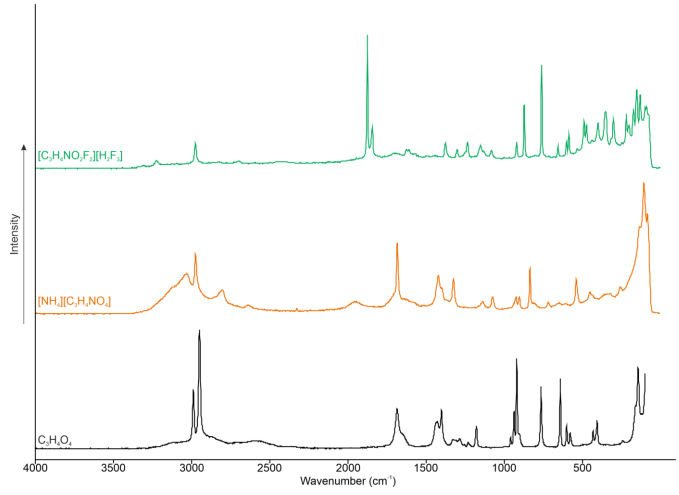

Figure 4
Low-temperature Raman spectra of $[C_3H_4F_2NO_2][H_2F_3]$, $[NH_4][C_3H_5NO_4]$ and malonic acid ($C_3H_4O_4$) (Hollenwäger *et al.*, 2024*b*).

4. Conclusion

Herein we present the first single-crystal X-ray diffraction and Raman spectroscopy study of the $[C_3H_4F_2NO_2][H_2F_3]$ salt. This salt represents the first difluoride in the group of diacylamino fluorides and is a further example of a complexone.

Acknowledgements

We are grateful to the Department of Chemistry at the Ludwig Maximilian University of Munich, the Deutsche Forschungsgemeinschaft (DFG), the F-Select GmbH, and Professor Dr Karaghiosoff and Dr Constantin Hoch for their support. Open access funding enabled and organized by Projekt DEAL.

References

Allen, F. H., Kennard, O., Watson, D. G., Brammer, L., Orpen, A. G. & Taylor, R. (1987). *J. Chem. Soc. Perkin Trans. 2*, pp. S1–S19.
Anderegg, G., Arnaud-Neu, F., Delgado, R., Felcman, J. & Popov, K. (2005). *Pure Appl. Chem.* **77**, 1445–1495.
Carpino, L. A. & Mansour, E. M. E. (1999). *J. Org. Chem.* **64**, 8399–8401.
Chaudhary, P., Goettel, J. T., Mercier, H. P. A., Sowlati–Hashjin, S., Hazendonk, P. & Gerken, M. (2015). *Chem. A Eur. J.* **21**, 6247–6256.
Farrugia, L. J. (2012). *J. Appl. Cryst.* **45**, 849–854.

Goettel, J. T., Chaudhary, P., Hazendonk, P., Mercier, H. P. A. & Gerken, M. (2012). *Chem. Commun.* **48**, 9120–9122.

Hollenwäger, D., Morgenstern, Y., Daumer, L., Bockmair, V. & Kornath, A. J. (2024*a*). *ACS Earth Space Chem.* **8**, 2101–2109.

Hollenwäger, D., Nitzer, A., Bockmair, V. & Kornath, A. J. (2024*b*). *Acta Cryst.* C**80**, 291–296.

Jeffrey, G. A. (1997). In *An Introduction to Hydrogen Bonding*. New York, Oxford: Oxford University Press.

Jiang, Q., Shtukenberg, A. G., Ward, M. D. & Hu, C. (2015). *Cryst. Growth Des.* **15**, 2568–2573.

Jin, A., Mack, H.-G., Waterfeld, A. & Oberhammer, H. (1992). *ChemInform*, **23**, 49.

Kollonitsch, J., Marburg, S. & Perkins, L. (1975). *J. Org. Chem.* **40**, 3808–3809.

Parsons, S., Flack, H. D. & Wagner, T. (2013). *Acta Cryst.* B**69**, 249–259.

Rigaku OD (2020). *CrysAlis PRO*. Rigaku Oxford Diffraction Ltd, Yarnton, Oxfordshire, England.

Sheldrick, G. M. (2015*a*). *Acta Cryst.* A**71**, 3–8.

Sheldrick, G. M. (2015*b*). *Acta Cryst.* A**71**, 3–8.

Spek, A. L. (2020). *Acta Cryst.* E**76**, 1–11.

supporting information

Acta Cryst. (2025). C**81**, 77-81 [https://doi.org/10.1107/S2053229624012452]

Monoprotonated species of 2-aminomalonyl difluoride, $[C_3H_4F_2NO_2][H_2F_3]$

Dirk Hollenwäger, Dominik Leitz, Valentin Bockmair and Andreas J. Kornath

Computing details

1,3-Difluoro-1,3-dioxopropan-2-aminium dihydrogen trifluoride

Crystal data

$C_3H_3F_2NO_2^+·H_2F_3^-$
M_r = 183.09
Orthorhombic, $P2_12_12_1$
a = 5.5736 (2) Å
b = 9.2154 (4) Å
c = 12.7952 (7) Å
V = 657.20 (5) Å^3
Z = 4
$F(000)$ = 368
D_x = 1.850 Mg m^{-3}
Mo $K\alpha$ radiation, λ = 0.71073 Å
Cell parameters from 2040 reflections
θ = 2.7–31.2°
μ = 0.23 mm^{-1}
T = 102 K
Needle, colorless
0.34 × 0.11 × 0.07 mm

Data collection

Rigaku Xcalibur Sapphire3 diffractometer
Radiation source: Enhance (Mo) X-ray Source
Graphite monochromator
Detector resolution: 15.9809 pixels mm^{-1}
ω scans
Absorption correction: multi-scan (CrysAlis PRO; Rigaku OD, 2020)
T_{min} = 0.945, T_{max} = 1.000
7118 measured reflections
2187 independent reflections
1930 reflections with $I > 2\sigma(I)$
R_{int} = 0.034
θ_{max} = 32.3°, θ_{min} = 2.7°
h = −8→5
k = −13→13
l = −19→18

Refinement

Refinement on F^2
Least-squares matrix: full
$R[F^2 > 2\sigma(F^2)]$ = 0.034
$wR(F^2)$ = 0.067
S = 1.02
2187 reflections
124 parameters
0 restraints
Primary atom site location: structure-invariant direct methods
Secondary atom site location: difference Fourier map
Hydrogen site location: difference Fourier map
All H-atom parameters refined
$w = 1/[\sigma^2(F_o^2) + (0.0296P)^2]$ where $P = (F_o^2 + 2F_c^2)/3$
$(\Delta/\sigma)_{max} < 0.001$
$\Delta\rho_{max}$ = 0.27 e Å^{-3}
$\Delta\rho_{min}$ = −0.18 e Å^{-3}
Absolute structure: Flack x determined using 683 quotients [(I+)-(I-)]/[(I+)+(I-)] (Parsons *et al.*, 2013)
Absolute structure parameter: −0.3 (5)

Special details

Geometry. All esds (except the esd in the dihedral angle between two l.s. planes) are estimated using the full covariance matrix. The cell esds are taken into account individually in the estimation of esds in distances, angles and torsion angles; correlations between esds in cell parameters are only used when they are defined by crystal symmetry. An approximate (isotropic) treatment of cell esds is used for estimating esds involving l.s. planes.

Refinement. Refinement of F^2 against ALL reflections. The weighted R-factor wR and goodness of fit S are based on F^2, conventional R-factors R are based on F, with F set to zero for negative F^2. The threshold expression of $F^2 > 2\text{sigma}(F^2)$ is used only for calculating R-factors(gt) etc. and is not relevant to the choice of reflections for refinement. R-factors based on F^2 are statistically about twice as large as those based on F, and R- factors based on ALL data will be even larger.

Fractional atomic coordinates and isotropic or equivalent isotropic displacement parameters (Å²)

	x	*y*	*z*	U_{iso}*/U_{eq}
F1	0.0476 (2)	0.32000 (12)	0.02215 (9)	0.0243 (3)
F2	0.4306 (2)	0.50434 (12)	0.05212 (8)	0.0244 (3)
O2	0.4408 (2)	0.58347 (13)	0.21402 (10)	0.0202 (3)
O1	−0.1665 (2)	0.31969 (15)	0.16660 (11)	0.0210 (3)
N1	0.2218 (3)	0.34495 (18)	0.29301 (12)	0.0171 (3)
C1	0.0210 (3)	0.33015 (19)	0.12529 (14)	0.0178 (3)
C2	0.3829 (3)	0.49451 (19)	0.15364 (13)	0.0160 (3)
C3	0.2606 (3)	0.35165 (19)	0.17959 (14)	0.0148 (3)
H1	0.154 (4)	0.257 (3)	0.3148 (19)	0.025 (6)*
H2	0.126 (4)	0.414 (2)	0.3121 (17)	0.020 (5)*
H4	0.362 (4)	0.275 (2)	0.1562 (15)	0.012 (5)*
H3	0.355 (4)	0.363 (3)	0.331 (2)	0.037 (7)*
F4	0.88392 (19)	0.54834 (12)	0.34615 (9)	0.0225 (2)
F5	0.53500 (19)	0.38358 (12)	0.59645 (9)	0.0221 (2)
F3	0.59728 (18)	0.39321 (12)	0.41590 (9)	0.0239 (3)
H5	0.784 (6)	0.482 (4)	0.378 (3)	0.071 (11)*
H6	0.562 (5)	0.385 (4)	0.524 (3)	0.070 (9)*

Atomic displacement parameters (Å²)

	U^{11}	U^{22}	U^{33}	U^{12}	U^{13}	U^{23}
F1	0.0236 (5)	0.0276 (6)	0.0217 (5)	−0.0004 (4)	−0.0047 (5)	−0.0041 (5)
F2	0.0234 (5)	0.0291 (6)	0.0209 (6)	−0.0026 (5)	0.0059 (4)	0.0023 (4)
O2	0.0194 (6)	0.0165 (6)	0.0247 (7)	−0.0033 (5)	−0.0023 (5)	0.0009 (5)
O1	0.0136 (6)	0.0208 (7)	0.0287 (7)	−0.0012 (5)	−0.0019 (5)	−0.0008 (6)
N1	0.0138 (7)	0.0171 (7)	0.0203 (8)	−0.0019 (6)	−0.0009 (6)	0.0030 (6)
C1	0.0185 (8)	0.0120 (8)	0.0227 (8)	0.0006 (6)	−0.0043 (6)	−0.0010 (7)
C2	0.0110 (7)	0.0176 (8)	0.0195 (8)	0.0006 (6)	0.0005 (6)	0.0027 (7)
C3	0.0120 (7)	0.0135 (8)	0.0188 (8)	0.0013 (6)	−0.0014 (6)	−0.0004 (6)
F4	0.0201 (5)	0.0205 (6)	0.0268 (6)	−0.0018 (4)	0.0006 (5)	−0.0004 (5)
F5	0.0238 (5)	0.0232 (6)	0.0193 (5)	0.0051 (4)	0.0010 (4)	0.0032 (4)
F3	0.0210 (5)	0.0301 (6)	0.0206 (5)	−0.0046 (4)	−0.0020 (4)	−0.0012 (5)

Geometric parameters (Å, º)

F1—C1	1.331 (2)	C1—C3	1.518 (2)
F2—C2	1.329 (2)	C2—C3	1.519 (2)
O2—C2	1.172 (2)	C3—H4	0.95 (2)
O1—C1	1.175 (2)	F4—H5	0.92 (4)
N1—C3	1.469 (2)	F5—H6	0.94 (3)
N1—H1	0.94 (2)	F3—H5	1.41 (4)
N1—H2	0.87 (2)	F3—H6	1.40 (3)
N1—H3	0.90 (3)		
C1···F4	2.676 (2)	C2···F5	2.688 (2)
C1···F5	2.682 (2)		
C3—N1—H1	112.9 (15)	O2—C2—C3	125.85 (16)
C3—N1—H2	109.8 (14)	F2—C2—C3	111.25 (14)
H1—N1—H2	107.6 (19)	N1—C3—C1	108.51 (14)
C3—N1—H3	113.6 (15)	N1—C3—C2	108.57 (14)
H1—N1—H3	109 (2)	C1—C3—C2	114.07 (14)
H2—N1—H3	103 (2)	N1—C3—H4	111.5 (12)
O1—C1—F1	122.64 (16)	C1—C3—H4	106.3 (12)
O1—C1—C3	125.94 (17)	C2—C3—H4	107.9 (12)
F1—C1—C3	111.40 (14)	H5—F3—H6	118.6 (19)
O2—C2—F2	122.80 (16)		
O1—C1—C3—N1	4.7 (3)	O2—C2—C3—N1	1.3 (2)
F1—C1—C3—N1	−173.50 (14)	F2—C2—C3—N1	177.71 (13)
O1—C1—C3—C2	−116.4 (2)	O2—C2—C3—C1	122.37 (19)
F1—C1—C3—C2	65.34 (19)	F2—C2—C3—C1	−61.17 (18)

Hydrogen-bond geometry (Å, º)

D—H···*A*	*D*—H	H···*A*	*D*···*A*	*D*—H···*A*
N1—H1···F5^{i}	0.94 (2)	1.84 (2)	2.7422 (19)	159 (2)
N1—H2···F4^{ii}	0.87 (2)	1.88 (2)	2.7426 (19)	172 (2)
N1—H3···F3	0.90 (3)	1.75 (3)	2.6551 (19)	174 (2)
F4—H5···F3	0.92 (4)	1.41 (4)	2.3221 (15)	170 (3)
F5—H6···F3	0.94 (3)	1.40 (3)	2.3378 (16)	177 (3)
N1—H1···F5^{i}	0.94 (2)	1.84 (2)	2.7422 (19)	159 (2)
N1—H2···F4^{ii}	0.87 (2)	1.88 (2)	2.7426 (19)	172 (2)
N1—H3···F3	0.90 (3)	1.75 (3)	2.6551 (19)	174 (2)
F4—H5···F3	0.92 (4)	1.41 (4)	2.3221 (15)	170 (3)
F5—H6···F3	0.94 (3)	1.40 (3)	2.3378 (16)	177 (3)

Symmetry codes: (i) *x*−1/2, −*y*+1/2, −*z*+1; (ii) *x*−1, *y*, *z*.